WiscWind

U.S. Department of Energy
2021 Collegiate Wind Competition
Technical Report

University of Wisconsin-Madison

Electrical Sub-team:	**Mechanical Sub-team:**	**Principal Investigator**
Justin Casleton *(EE Team Lead)*	Zak Schuster *(ME Team Lead)*	Scott Williams
Michael Schmich	Carter Pryzbylski	
Ian Bormett	CJ Bajaj	**Faculty/Staff Advisors:**
Kyle Kryzer	Zhengjia Mao	Randy Jackson
Zach Berglund		Kyle Hanson
Truman Kent		
		Contact
		spwilliams@wisc.edu

Table of Contents

Executive Summary

WiscWind is an interdisciplinary engineering student organization competing in the U.S. Department of Energy 2021 Collegiate Wind Competition (CWC), giving students real-world experience in the growing renewable energy industry. The mechanical and electrical sub-teams are tasked with designing and fabricating a wind-driven power system that maximizes power generation and can accomplish specific tasks detailed in the competition rules.

The mechanical sub-team completed research on last year's design to improve results from the 2020 competition. The major tasks this year have mainly focused on the implementation of an active pitch control system, while secondary focuses have been identified with improvements of the blade design and yaw control design. These factors have been worked on to improve the mechanical efficiency of the turbine. This will allow a greater speed of the shaft for a given wind speed, which creates a greater power output, as well as better control over the speed of the shaft throughout any wind speed range to help maintain a good power output. With greater control over the power output of the turbine, the team would have scored higher marks in the many categories of the wind tunnel test of the 2019 competition, which was our latest active competition due to COVID-19. The fall semester was dedicated to further research, preliminary testing and implementation of the new blade designs, with development and implementation of the pitch and yaw controls in the spring.

The electrical sub-team focused on converting the mechanical energy captured by the wind into electrical energy. This year the team decided to use the generator that was manufactured last year but was not able to be tested. Emphasis on testing and possible improvements allowed the team to focus more attention on the power electronic circuits to control high efficiency three-phase AC to DC conversion, electrical noise suppression, emergency load disconnection, and emergency braking using an ESP 32 microcontroller and a combination of hand-built and off-the-shelf circuitry. The fall semester was dedicated to verifying the generator as well as coordinating with the mechanical team about the active pitch control. The spring semester was dedicated to the creation of new braking and voltage regulation systems in order to meet the requirements of the competition. These systems were designed and verified piece by piece in a distributed team environment.

Our mechanical and electrical designs have been an iterative process. All parts had been purchased, machined, and assembled by members of the team. Most components have been tested individually both in the wind tunnel and on the dynamometer. The prototype of our turbine was run through a majority of the competition tests prior to the writing of this report, though some aspects of the competition remain untested due to a large number of our team graduating and beginning work, some members leaving the campus area for the summer, and an unforeseen deconstruction for maintenance on the campus wind tunnel for the first 2 weeks of May. The tests that the team had been able to complete had promising results that lead us to believe that we would have been able to be very competitive against others in the competition.

Introduction

WiscWind's development and design for the Collegiate Wind Competition's prototype turbine focused on optimizing performance and maximizing the turbine power output over all wind speeds. This is largely achieved through the team's successful implementation of an active pitch control system, which helps better control the turbine throughout all of the competition testing tasks. Converting the mechanical energy captured by the wind into electrical energy is accomplished with a custom-made three-phase axial flux generator. Power electronics circuits control AC to DC conversion, power regulation, and emergency braking. Iterative testing validated our design choices to meet the needs of the competition.

Mechanical

Mechanical Design Objectives

WiscWind's top priorities for the mechanical design this year largely focused on the implementation of an active pitch control system. As previously discussed, this system would help give better control over the turbine throughout all of the competition testing tasks, but specifically help the turbine succeed during the Rated Power and Speed, Durability, and Safety testing tasks. The system reads the rotational velocity on the shaft using a photo encoder and adjusts the pitch angle to either keep the rotational velocity as close to constant as possible for rated power or to limit the rotational velocity at high wind speeds when the turbine is at risk of failure. This system also can be triggered to pitch the blades completely out of the wind, thus reducing the rotational velocity by a drastic amount. The blade geometry was made robust to ensure fracture does not occur along the base of the blades, where the pitching occurs, and to ensure the blades could survive any angle of attack from the wind they may encounter. While there are many other subsystems of the wind turbine including the yaw control, nacelle, and tower subassemblies, they do not have as much of an impact on the desired performance abilities of the wind turbine as the blades and control systems. A CAD model and assembly of our prototype wind turbine can be seen in Figure 1 below.

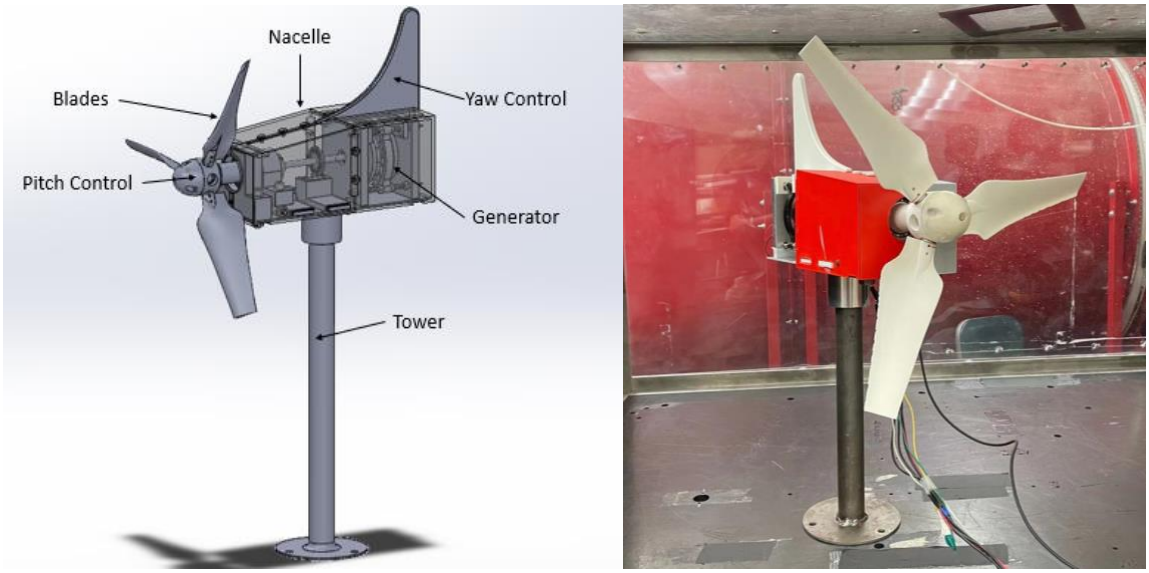

Figure 1. (L) Turbine prototype CAD model; (R) Prototype turbine assembly in wind tunnel test.

Turbine Blades

Research Concepts

A reliable and effective blade design contributes significantly to maximizing the efficiency of a wind turbine. The sole purpose of a turbine blade is to extract as much energy from the wind as possible, which can be done by separating the design into two main aspects: aerodynamic and structural design. Inevitably, the two aspects interact and often contrast each other, but both are essential to consider while developing an effective blade design [1]. The aerodynamic portions of turbine blade design encompass the selection of optimal geometry for the external surface of the blade, which is defined by the airfoil structure, the twist, and the thickness distributions throughout the entire chord length. The main objective for an aerodynamic blade design is to maximize the energy yield, while also helping limit the maximum power output if necessary.

The main portion of the aerodynamic design is based upon airfoil selection, which is of the utmost importance when considering the efficiency of a turbine blade. The first step taken to research airfoil designs was to investigate the success of past airfoils in the Collegiate Wind Competition. As WiscWind's previous team had identified, teams who had used the Wortmann FX 63-137, shown in Figure 2, would typically finish towards the top of previous competitions, so it was decided to keep the design between the two years similar, though this year we increased the blade chord in numerous areas to help increase the surface area in contact with the wind.

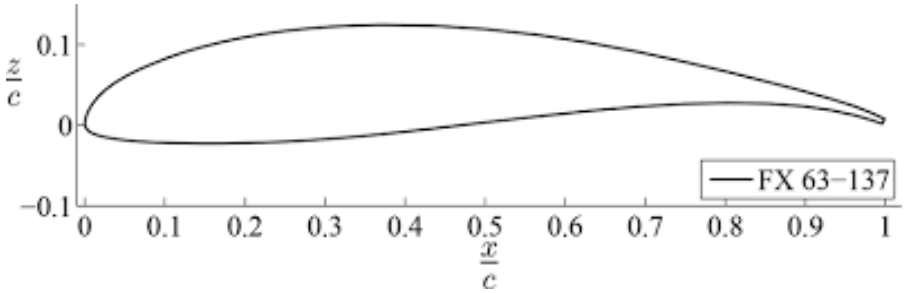

Figure 2: Wortmann FX 63-137 airfoil [2].

The Wortmann FX 63-137 airfoil has been commonly used for small scale turbine applications, as it is known to have a high efficiency at laminar flow, though efficiency takes a large hit when introduced to turbulent flow due to large drag forces [4]. The type of flow can be determined through the calculation of the Reynolds' number, which can be found using the equation shown in Equation 1:

$$Re = \frac{\rho v L}{\mu} \quad (1)$$

where L is the chord length of the airfoil for a turbine blade, ρ is the air density, ν is the wind velocity, and μ is the air viscosity. The air density and the viscosity at the testing site in Indianapolis as well as the range of testing wind velocities are known values, so we can approximate the Reynolds' number to be in a range of ~10000 - 40000, which will be in the laminar flow region. The Wortmann FX 63-137 excels within the laminar range and thus supports the selection of this airfoil for use on our small-scale turbine [3]. To promote the best cut-in wind speeds and maximum efficiency of the blade, a large chord length with a large angle twist at the root of the blade is ideal, whereas a smaller chord length with a small angle twist towards the tip of the blade is ideal.

The structural portions of turbine blade design depend on blade material selection and the determination of a structural cross section. The structural integrity of the blades must be sufficient to withstand the range of wind speeds that they will come into contact with. For purposes of the competition,

it had been requested that blades could handle wind speeds up to 25 m/s. The forces upon the blades can be estimated using Equation 2:

$$F_w = \frac{1}{2}\rho v^2 A \quad (2)$$

where F_W is the wind force, rho is the air density, v is the wind speed, and A is the surface area of the blade in contact with the wind. The air density and maximum value of wind speed are known, and with an estimate of the blade area, the range of the wind force that the blade can experience can be determined to be between 2-6 N, depending on the surface area in contact with the wind. It is essential that the blade be able to withstand this force without structural failure, which depends on material selection. To produce strong blades for testing, while also remaining cost-effective, the ABS material printed on the Stratasys printer was used for blade production. This material has an ultimate strength of around 40 MPA, which was more than sufficient for testing with competition parameters.

Blade Design

Using the knowledge gained throughout the research of the turbine blade design, a blade was designed similar to last year's design, though with a larger chord length distribution to help maximize the surface area of the blades in contact with the wind. The twist distributions of the blade came from the results of the previous year. The overall blade length has been selected to take up as much space as possible within our 45x45x45cm confinement for the competition, hoping to convert the maximum amount of energy from the wind. Figure 6 shows the geometric distribution of the testing blades.

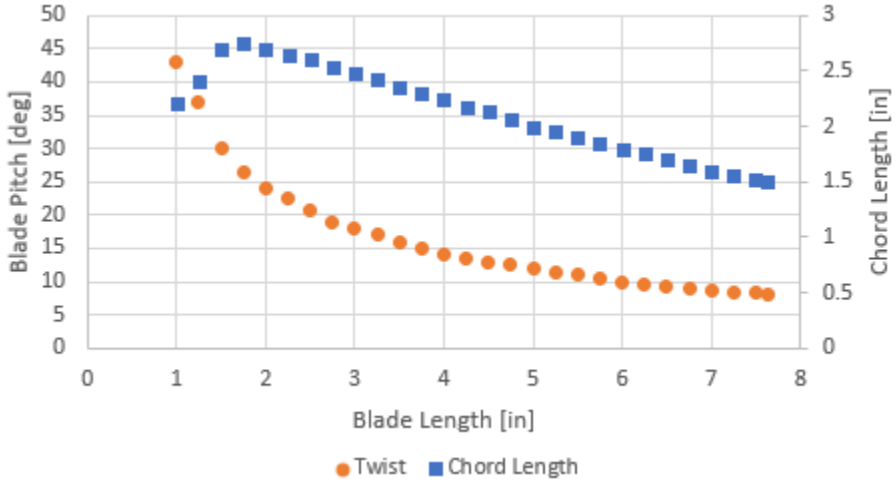

Figure 6: Blade chord length and twist distributions for initial testing blade.

The blades were designed in Solidworks using a loft feature, of which the profiles are shown in Figure 7. A connection point between the blades and the pitch control was added to the root of the blade, which completed the blade design, which is also shown in Figure 7.

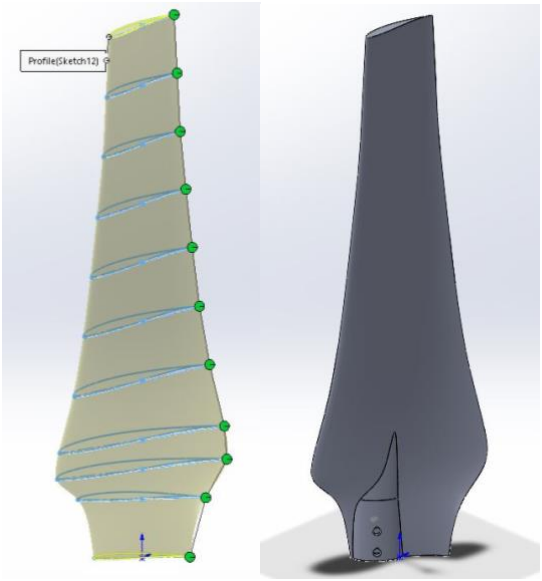

Figure 7: Optimized blade profile (L) and completed blade design (R).

Blade Analysis

After the addition of the connection point between the pitch control and the blades, a finite element analysis (FEA) was run on the blades to ensure that the blade could withstand the forces from both a headwind and crosswind orientation. The headwind orientation represents the direction wind is expected to approach the blade at higher wind speeds, when the force acting upon the blade will be at its highest. The crosswind orientation represents the worst angle for the wind to approach the blade, as this orientation has the wind force acting upon the thinnest portions of the blade, the most likely orientation that would cause the blade to fracture. This orientation was used for structural analysis to ensure the blade could handle the maximum wind speed that could be applied to the blade. At 25 m/s, the maximum wind force applied to this blade could be estimated to be around 3.75 N. The maximum stress encountered by the blade in either wind orientation is around 2 MPa, which is significantly less than the Ultimate Tensile Strength of ABS, 40 MPa. The tip of the blade moves the most when the wind force is applied, and with the tip of the blade will move 0.7 mm in the headwind orientation, and up to 1.6 mm in the crosswind orientation. The Von Mises stresses from the analysis are shown in Figure 8, and the displacement from the analysis is shown in Figure 9.

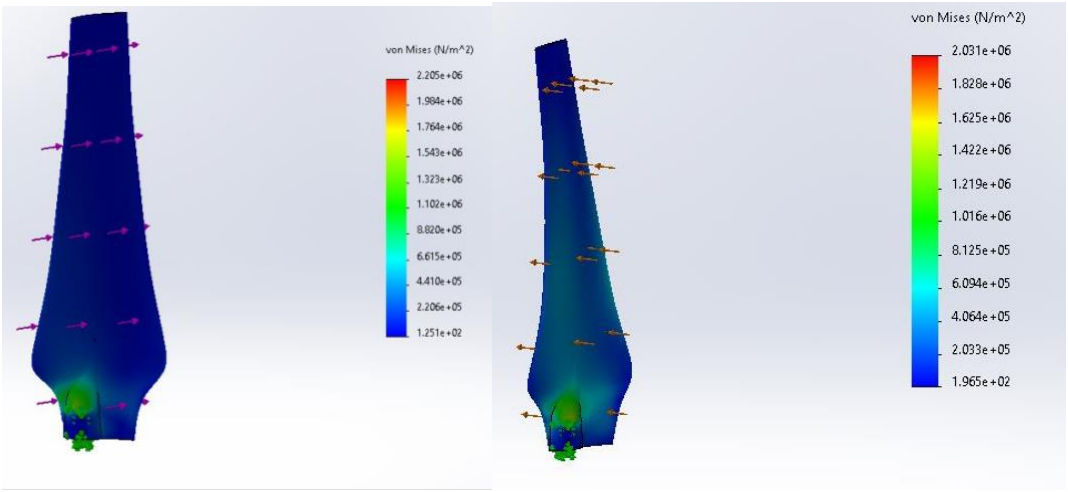

Figure 8: FEA Von Mises results for headwind (L) and crosswind (R) configurations.

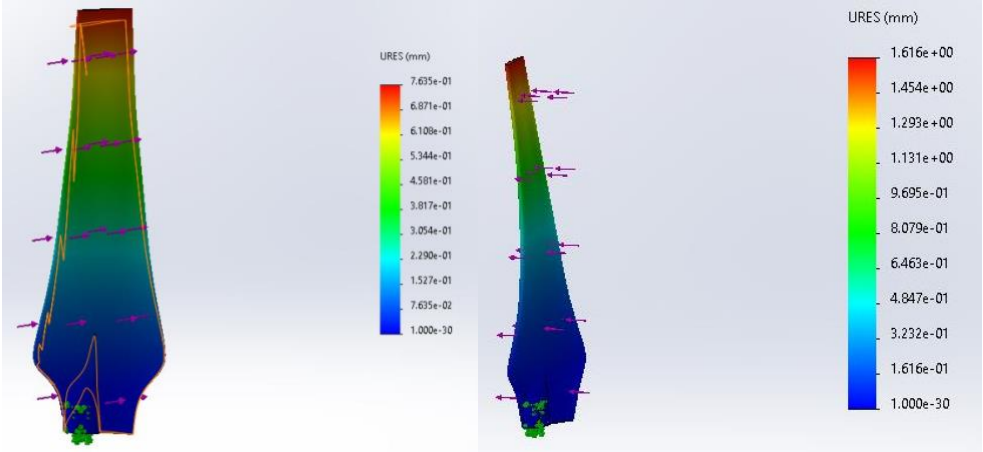

Figure 9: FEA displacement result for headwind (L) and crosswind (R) configurations.

Blade Manufacturing

Prototyping of these blades proved to be initially difficult due to the extremely thin contours along the trailing edge of the blade. The on campus Stratasys printer had trouble printing this portion of the blade in a lengthwise manner, which was the most efficient and cheapest way to print these blades. The left image in Figure 10 shows the fraying of material along the trailing edge when printed in this manner. To correct this, the team printed the remaining blades in a widthwise manner. This more than doubled the cost of the blades each time printing was needed but resulted in a much better surface quality along the trailing edge of the blades, as shown in the right image of Figure 10.

Figure 10: Blade quality from 3D Printing with ABS Material, lengthwise (L) and widthwise (R).

Pitch Control

Design Concept

The idea of an active pitch control system was initiated last year but the team was not able to complete their conceptual design. Our team designed an active pitch control system that is based on the movement of a linear actuator, which is connected to a triangular pinion that actuates the three blades by rotating gears mounted to the root of the turbine blades, shown in Figure 11. This system allows the blades to rotate up to a maximum of 90 degrees, which is more than enough to influence the effect the wind has on the blades and rotational velocity of the shaft. The triangular pinion has only two degrees of freedom: moving forward or backward, which is controlled by the linear actuator.

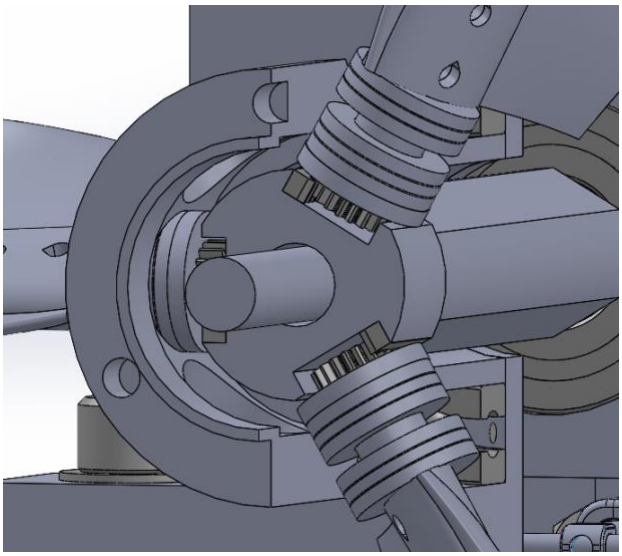

Figure 11: Gears mounted to the root of the blades that rotate upon linear movement of the triangular pinion.

To explain the functionality of this system, it can be split into 3 separate sections, highlighted in Figure 12. The first section, the hub and support system, consists of the hub, blades, support mounting block, and support ball bearing. This design helps support the front of the turbine and allows for free rotation of the hub and associated internal components without allowing any linear motion of the system. The second section, the pitch control mechanism, consists of the triangular pinion, actuator mounting block, actuator ball bearing, adjustable collar, and the linear actuator. This system can freely rotate with the hub and blades, but also has the additional degree of freedom to allow for linear movement, which corresponds to the movements of the fixed actuator. When the actuator extends, the blades begin to close off from the wind, and when the actuator retracts, the blades begin to open up again. The final section, the driveshaft, consists of the nose and driveshaft. This section can rotate freely with the hub and is fixed in place by a coupler that is connected to the generator. This coupler restricts linear movement and helps keep the generator rotating at the same speed as the driveshaft.

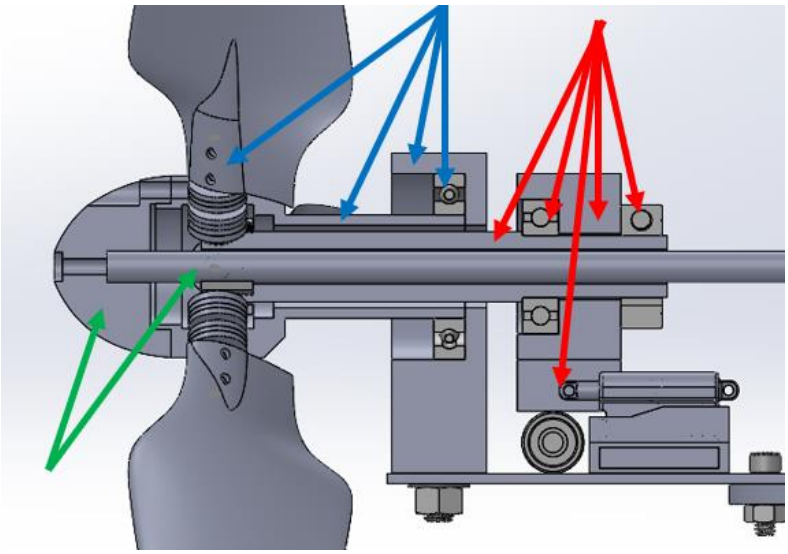

Figure 12: Pitch control mechanism sections. The hub and support system is identified in blue, the pitch control mechanism is identified in red, and the driveshaft is identified in green.

Practical Implementation

The pitch control subsystem is designed and assembled based on the diagram as shown in Figure 13. It mainly consists of a power source, a microcontroller, a photo encoder, and a linear actuator & LAC board.

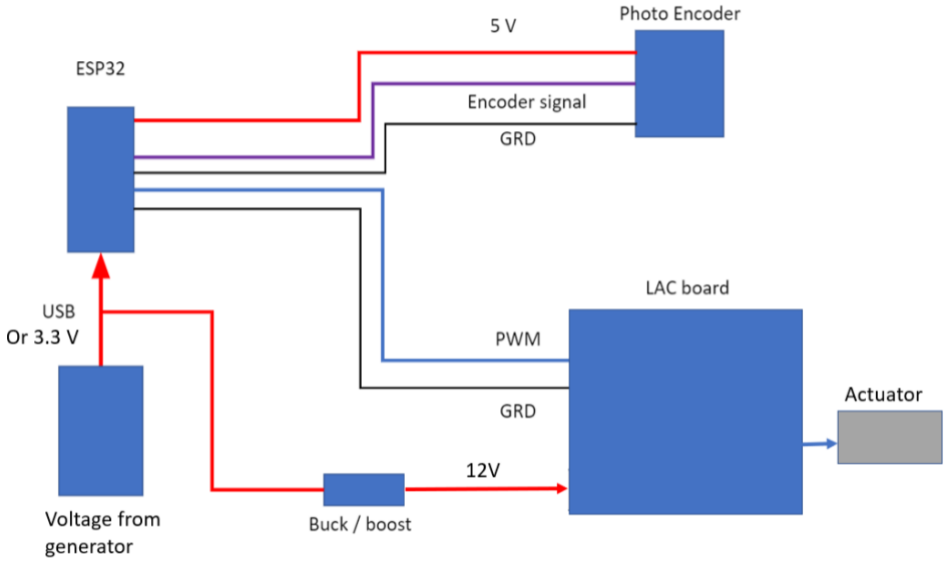

Figure 13: Pitch control wiring diagram.

An Actuonix PQ12-P linear actuator with feedback, as shown in Figure 14, is used to move the highlighted cylinder mentioned above forward or backward. The actuator has a 100:1 gear ratio and a max operating voltage of 12V, and it produces up to 50N force and 20mm stroke length. An Actuonix Linear Actuator Control (LAC) board, as shown in Figure 15, directly connects and evokes the actuator. The LAC board and the actuator are powered with 12V, drawn from the generator through a power regulator, while the ground and signal wires are connected to a Adafruit ESP32 microcontroller. The microcontroller sends PWM signals to the LAC board to manipulate the distance that the actuator extends or retracts, and the distance is linearly related to the duty cycle percentage of PWM signals.

Figure 14: PQ12-P Linear Actuator with Feedback

Figure 15: LAC Board

The microcontroller also powers a WYC-H206 photo encoder, as shown in Figure 16, and reads RPM from it. The photo encoder measures the rotational speed of a plastic wheel that is mounted on the main turbine shaft, as shown in Figure 17. The wheel has 40 spaces that allows the laser to pass through and generates a pulse in the encoder. The microcontroller counts the number of pulses in a given time interval and calculates the RPM. Based on the RPM, the microcontroller determines whether the blades need to pitch. If the RPM is above the threshold, the microcontroller sends a PWM signal with higher duty cycle percentage that pitches the blades partially out of the wind to reduce the loading. Otherwise, the

microcontroller keeps sending a default PWM signal with constant duty cycle percentage. Lastly, the microcontroller is powered with 3.3V drawn from the generator. Once the wind speed is above the cut-in wind speed and the turbine begins to rotate, the generator quickly produces enough power to evoke the microcontroller. The actuator, encoder, and encoder wheel are identified in Figure 18.

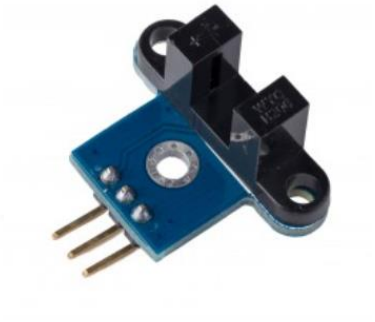

Figure 16: WYC-H206 Encoder

Figure 17: Wheel with 40 spaces

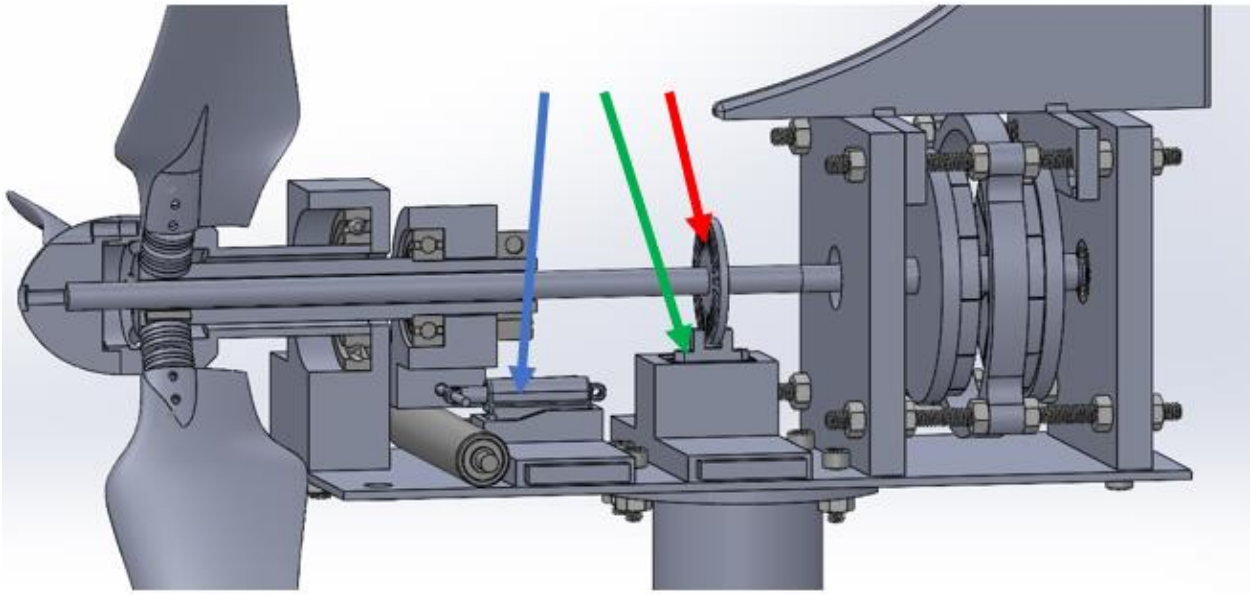

Figure 18: Actuator (blue), encoder (green), and encoder wheel (red) identified within the prototype CAD model.

Pitch Control Script

The software implementation of the above process is achieved through Arduino IDE. The script in the Appendix A is uploaded to the microcontroller, and it is capable of executing the same script as long as it is connected to power. However, one problem from testing was that the current photo encoder does not have enough resolution to read the rotational speed more than 256 RPM. It displays the rotational speed as 4 RPM if the actual speed is 260 RPM, and such a resolution problem happens for every 256 RPM. Therefore, a simple algorithm is added to the script to solve the resolution problem. The complete version is included in the script.

While this algorithm solves the resolution problem, it also exposes additional limitations to RPM measurement. This algorithm only works when the wind speed is gradually increased or decreased so that

it keeps track of the multiplier. Because the script collects RPM for every 1000ms, any RPM jump larger than the threshold range under high wind speeds will lose track of the multiplier. For example, if the old_rpm is below our customized threshold of 200 and the new_rpm is above 60, the "if" statement will be skipped and the multiplier will not be incremented. Changing the threshold range will also bring new limitations. Therefore, getting a new encoder with a higher resolution to output a single RPM reading will be ideal for future improvements.

Nacelle and Yaw Control

The main function of the yaw control system is to rotate the nacelle to keep the turbine blades facing into the wind, where the maximum amount of wind energy can be converted into rotational energy on the driveshaft. Investigating research from previous competitions reassured the team that a passive system would be sufficient for the competition. Much of the research suggested that both active and passive yaw control systems have similar performance capabilities at the small-scale application. An active system would require a closed loop feedback system that would draw some power generated by the turbine, thus inhibiting the total net power generated. The passive system would require a smooth bearing rotation to properly orientate the turbine and need a well-rounded design with an abundance of useful surface area for wind contact, while also remaining lightweight. The team decided to proceed with a passive yaw control system to help maximize the power generation of the turbine.

Next, research was done to determine the most suitable shape for the yaw tailfin, which is responsible for correcting the nacelle position. The ultimate goal is to maximize the force exerted onto the tailfin by the incident wind since overshoot is not a concern at this scale. A study on microturbines performed CFD on three different fin shapes (rectangle, triangle, and trapezoid) with four different incident wind angles (0, 10, 20, and 30 degrees), with a fixed wind velocity of 7 m/s. The study found that the triangular fin had more force exerted on it at each of the four angles, shown in Table 1.

Angle of Inclination (degree)	Forces(N) acting on		
	Rectangular Tail	Trapezoidal Tail	Triangular Tail
0	0.00106	0.00113	0.00196
10	0.00557	0.00574	0.00660
20	0.02797	0.04420	0.05280
30	0.07152	0.07551	0.07759

Table 1: Force exerted on microturbine yaw tailfin [4]

Based on this research, a triangular geometry was chosen as the yaw fin's starting point. Based on WiscWind's past yaw designs, having a top and bottom fin seemed to be overdesigned. The incident wind hitting the bottom fin generally does not exert much force since it is being obstructed by the tower. The design from this year only consists of a top, triangular fin since this has no obstructions except for the blades, making it equally effective but simpler. The initial tailfin was made in Solidworks and resembles that of an airplane. This design does not have many complex contours or splines for easy manufacturing. Even the fillets are dimensioned to be easily manufacturable. Figure 19 shows the tailfin design with a top and bottom structure, made by the 2020 WiscWind team, and Figure 20 shows the 2021 simplified fin concept.

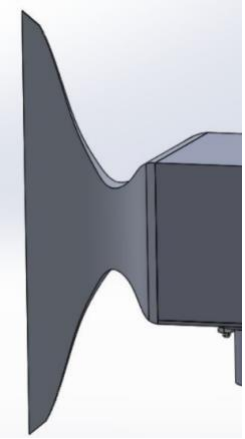

Figure 19: 2020 team's fin design

Figure 20: 2021 team's simplified fin concept

The initial yaw control design included the yaw fin as seen in Figure 20, along with the mounting structure. The mounting structure has a rectangular cross section, like the generator back plate, with 4 threaded holes which will be used to mount the yaw control. While evaluating analysis methods, it seemed best to not do a CFD analysis because the yaw control is situated at the back of the turbine so the fluid flow around it would be uncertain. Usually, the passive design has no functionality issues, so a simple FEA was done. The FEA was done multiple times to help achieve a good initial design (3D print-worthy) by eliminating critical stress concentrations. The latest FEA results can be seen in Figures 21 and 22.

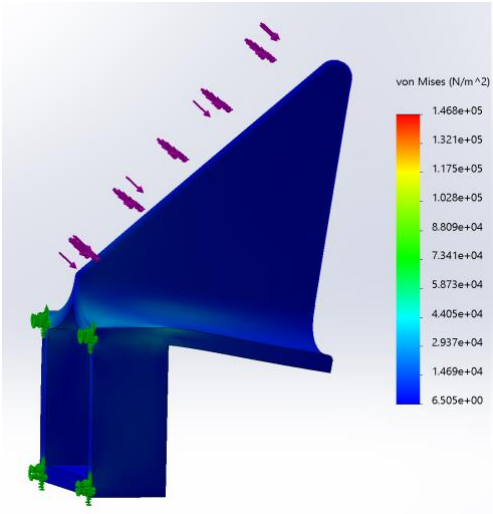

Figure 21: FEA results for loading case 1

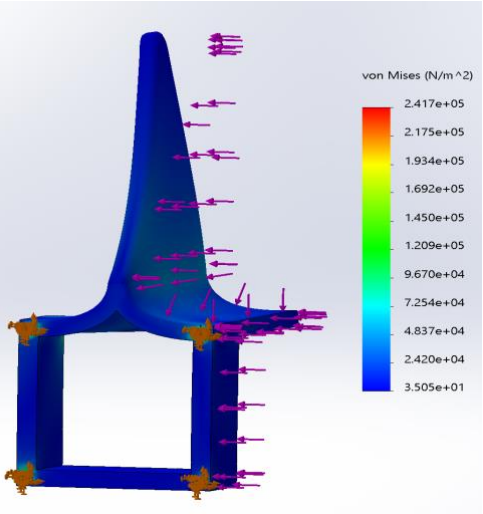

Figure 22: FEA results for loading case 2

For FEA, two loading conditions were chosen, and the forces applied were the maximum forces exerted by 25 m/s wind. The analysis was done on Solidworks and the material chosen was PLA plastic. PLA is strong, cost effective, and readily available for 3D printing, making it an easy selection. The first loading case represents the fluid (wind) force exerted onto the front of the fin when the turbine is correctly aligned with the wind. Low stress is especially important in this case because this is going to be the most common loading that the fin will experience. The second case shows the force exerted onto the side of the fin, representing a 90-degree angle of incidence. This is the case when the turbine is misaligned and needs to "yaw" into the correct position. The actual angles of incident wind will be less than 90 but worst case FEA was done, and the force exerted is the greatest at 90 degrees since the surface area normal to the wind is maximum at that angle. The FEA shows that PLA would be a suitable material for this design, since the

maximum stress in any of the cases is much less than the yield strength of PLA, with a safety factor much greater than 10. Next, this design was 3D printed for prototyping and further optimization.

The final yaw control design was changed significantly from the phase 2 design, optimized and accounting for the pitch control design and the other turbine components. The final design consists of a curved, triangular geometry which will maximize surface area and shift its center of mass more towards the back, allowing for greater rotation. This design is mounted right on top of the generator rather than towards the back of it, since the total length of the other components increased, and we are constrained to the 45 cm cube. A slotted path was created in mounting of the yaw control which will allow it to easily slide onto the bolts in between the generator plate as well as for ease of removal. This can be seen in Figure 23.

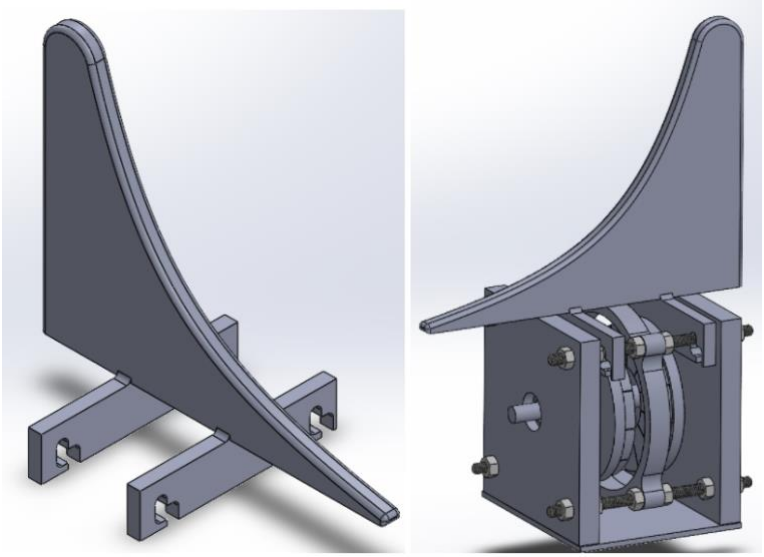

Figure 23: Yaw Control Design (L) and its mounting/assembly (R)

For structural analysis, worst case FEA was conducted in the headwind and crosswind orientations. These results confirmed our material selection since it had a safety factor of between 5-10 depending on the infill. The yaw control should not yield, and the maximum deflection was 0.5 mm, which the design will easily be able to bend under the CWC design loading condition. Based on that we decided to 3D print the design using 40% infill PLA since it had a good surface finish and was relatively light. The printed part, due to the nature of additive manufacturing, did not have great tolerances. This led to a slightly uneven part which was not perfectly flush with the generator bolts. Nonetheless, we designed the back portion of the nacelle to push down on the yaw control, forcing it to be flushed and locked into place.

Electromechanical

Electromechanical Design Objectives

The generator was designed with ease of manufacturing, assembling, and maintenance in mind, while also attempting to keep friction extremely low and allowing it to be contained in one concise package for use on different turbine chassis in the future. Electrically, the generator was designed to have minimal cogging torque, create enough voltage at low speeds to remove the need for a gearbox, have large enough gauge wires to ensure high power output, and create balanced three-phase power.

The three-phase axial flux generator designed for the 2020 competition was completed in March 2020. This meant that last year's team was unable to conduct thorough testing to verify the design upgrades that they had made. Because of our team's initial small size and ongoing restrictions to shop space, our

team decided to utilize the work of our predecessors and focus our efforts on testing and improving. The generator was tested using a dynamometer with different resistive loads to get accurate power curves for load selection. The final design was tested multiple times and a 200-ohm load was selected as the competition load for the turbine. The results of this dynamometer testing can be found in Appendix B.

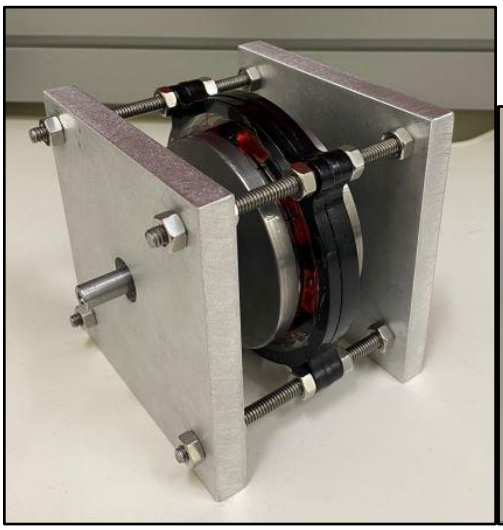

Figure 24: Fully Constructed Generator

Figure 25: Generator Stator and Two Rotors

Generator Improvements

The team first investigated potential modifications to improve generator performance. A patent from 2001 was found to be relevant to reducing flux leakage in electric generators. This patent focused on a cored axial flux generator, which is unlike ours, however it can be assumed that the principles used in their design will hold as the important properties only have to do with the interactions between the rotor magnets. The principles of this generator design come from what is known as a Halbach array, which can be seen in Figure 26.

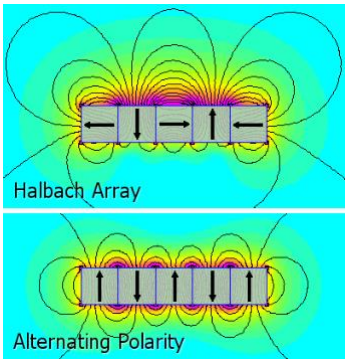

Figure 26: Magnetic Field of a Halbach Array versus Alternating Polarity Magnets [5]

Our current generator layout uses an alternating polarity design, which is the most common design. In theory, using the principles of a Halbach increases magnetic flux flowing through generator coils, as seen by the increased arcs of the magnetic field lines in Figure 26. The increase in flux provided would increase the voltage, and thus power output, of our generator. In an effort to simply improve on last year's

design and avoid re-manufacturing the generator, we modified this idea. Our team hypothesized that placing magnetic stripping around the outside of the rotor would act in a similar manner and decrease the flux leakage through the circumference of the rotor. Results from this experiment can be found in the Testing section.

Electrical

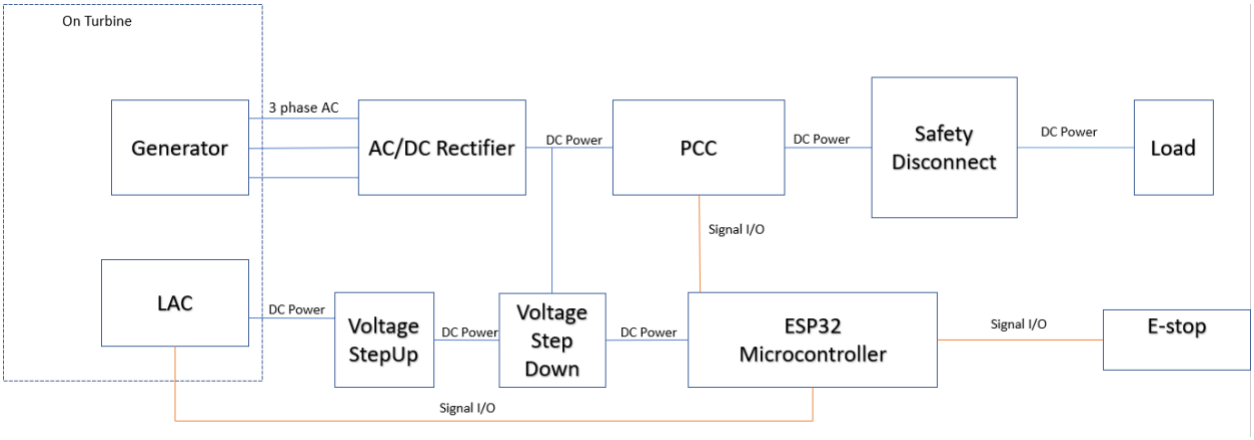

Figure 27: 2021 Electrical One Line Diagram

Introduction

Choosing to use the generator from 2020 allowed the electrical team to focus on other systems in 2021. With the competition goals in mind, the team developed a voltage regulation system to power both the microcontroller and active pitch control, as well as a braking system to meet the safety requirements of the competition.

AC/DC Conversion

Since our generator produces 3-phase AC power, it must be converted to DC for both competition data collection as well as our power electronics. The 2020 team utilized the Linear Technology DC2465 board for AC to DC conversion. On the board, there are three LT4320 IC's, which are ideal diode bridge controllers that drive six low loss N-channel MOSFETs to tell when they are on and off. The FETs are used as switching regulators, which turn on automatically without any voltage drops. This design dramatically reduces power and voltage losses. It enables the overall system to be specified to operate with a smaller, more cost-effective power supply due to the enhanced power efficiency. Low voltage applications benefit from the extra margin afforded by saving the two diode drops inherent in diode bridges. Compared to traditional approaches, the MOSFET bridge enables a rectifier design that is highly space- and power-efficient. We found the DC2465 board to be an appropriate choice for our needs again this year and felt that using a proven solution for AC to DC conversion allowed our team to focus on other areas.

Voltage Regulation

The voltage regulation system is vital to ensuring that our ESP32 maintains the appropriate voltage as well as providing adequate power to the Linear Actuator Control board. The ESP32

microcontroller expects a 3.3V input while the Linear Actuator expects a 12V power supply. To tackle this problem our team decided to use a two stage Buck/Boost system. The first stage is a Pololu D36V50F3 Step Down Voltage Regulator which can take an input of 4.5 to 50V and reduce it to the 3.3V required by the ESP32. The second stage consists of a Pololu U3V50F12 Step Up Voltage Regulator which accepts an input voltage of 2.9 to 12V and outputs the 12V required by our Linear Actuator. Both were chosen because they were low-cost solutions that had appropriate input ranges and were designed to handle an adequate current for our system.

Once the two boards arrived, the system was tested as outlined in the distributed manufacturing milestone. This process focused on iterative testing. First, each board was verified to operate as expected on its own. Once that was done, the two were configured in a similar manner to the final layout and tested using a benchtop power supply. After our team was satisfied that this method would protect our other components while also providing them appropriate power, they were assembled into the turbine testing setup as outlined in Figure 28. The final voltage regulation system was tested with the turbine in the wind tunnel to test the extra load it would pose on the generator, as the linear actuator was then being powered by the generator output. Wind tunnel testing proved the concept and allowed for continued control of the linear actuator to control the pitch of the blades at decent speeds. The extra power draw from the generator did pose an extra load on the system, which showed slightly reduced voltage measurements at the varying wind speeds.

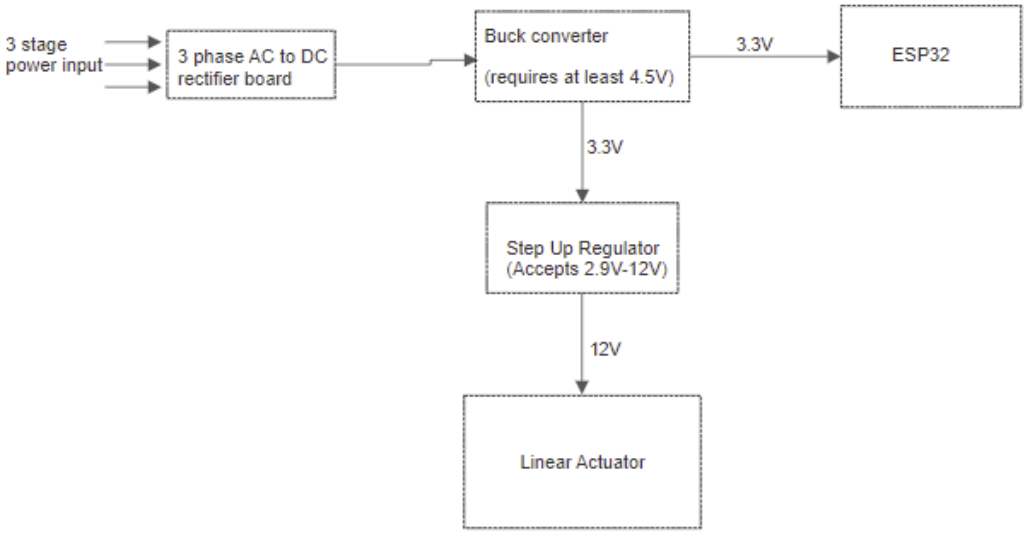

Figure 28: Voltage Regulation System

Safety and Braking

The braking system was originally designed to make use of an DPDT relay to switch between our competition resistive load of 200 ohms and the braking load of 1 ohm. Switching from the 200-ohm load to the 1-ohm load torques the generator to slow the blades. As discussed in previous competition milestones, the method of braking was slightly adapted as well as the blade connections to the shaft. After testing the first design in the wind tunnel, it was decided that the blade connections required more structural integrity to hold up to braking at higher speeds in the wind tunnel (9 m/s +). The mechanical pins connecting the blade to the rotating shaft were then made out of aluminum to increase the strength

over a PLA 3D printed material. After the mechanical improvements were made to the blade connection points, the new braking system was able to be tested with confidence.

Originally, the braking system was going to be activated by a control signal sent from an E-Stop button to engage the braking system. The control signal would be received by the ESP 32, which would then run the braking script where the braking load would be switched to using the DPDT relay. The system in theory would also be able to read a voltage input and engage the braking script automatically once close to the competition limit of 48 VDC. This plan was developed and partially tested but was not implemented fully in the end due to lack of time. The final braking system consisted of a Panasonic SPST power relay to manually switch on a 1-ohm resistor in parallel with the 200-ohm competition load. When the switch is in the open position, the power runs through just the 200-ohm load and when the switch is closed, the power runs in parallel through the 1-ohm and 200-ohm resistive loads. This creates a combination ~1 ohm which provides significant braking potential for the generator. The new braking subsystem was first tested in the lab with a bench top power supply and the normal electrical setup before being fitted for the wind turbine.

Testing and Results

Testing of Generator with Magnetic Strips

The Mechanical Team found research that supported the use of magnets or magnetic stripping to reduce flux leakage from an axial flux generator. The most ideal implementation of the magnetic stripping would be between the generator coils (inside the epoxy resin that holds the piece together). This implementation was not possible without destroying the previous year's generator design and starting over. Instead, the electrical team tested the generator by putting magnetic stripping around the outside of the stator (coils). The testing was conducted in a lab setting with a bench top power supply on a dynamometer, which is useful for consistent testing of the generator assembly. After testing the generator at different speeds, with different resistive loads, the results showed that there was not any big difference between the test with the magnetic stripping and that without. It was concluded that this implementation would not work for this year's system but could be a consideration for future improvement.

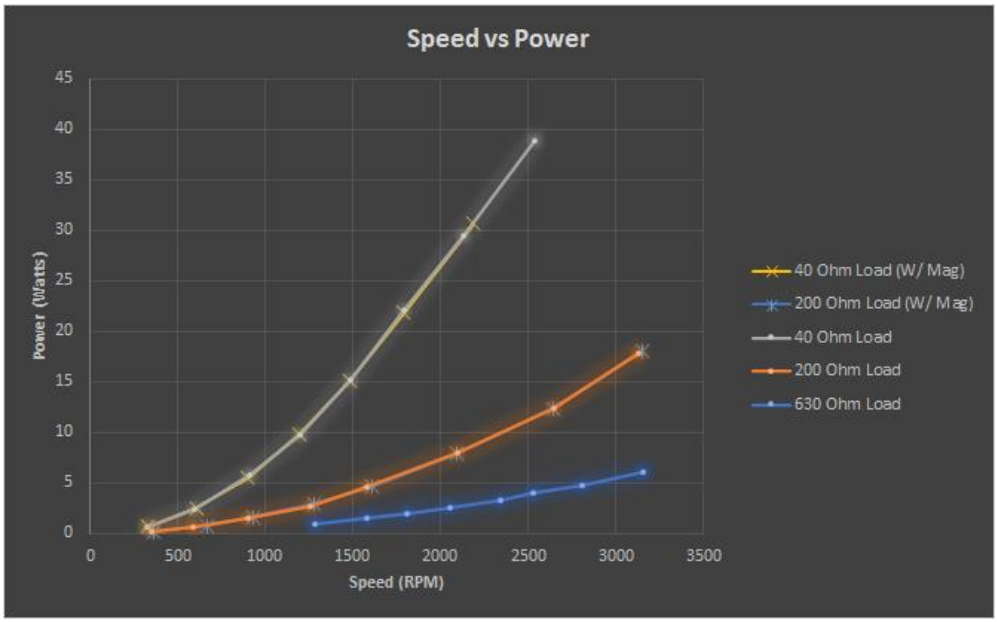

Figure 29. Speed vs Power representation of magnetic strip generator testing

Testing of Emergency Braking

The braking system was tested at various different wind speeds from 5 m/s up to 11 m/s and performed as expected in all cases. The changing of the load resistance with the braking system proved to be quite effective in reducing output power and also in reducing the speed. The power figures shown below are an accurate depiction of the braking capabilities of the turbine system in terms of its stopping ability. Due to a late switch in the system and also construction that was happening on the wind tunnel, RPM measurements were not able to be taken. A significant reduction in speed was observed and is presumed to be under the 10% operating speed. Competition rules dictate that the turbine speed must be reduced to less than ten percent of rated value. Figure 30 below shows the ability for the generative braking to reduce the wind turbine speed and power as the competition requires.

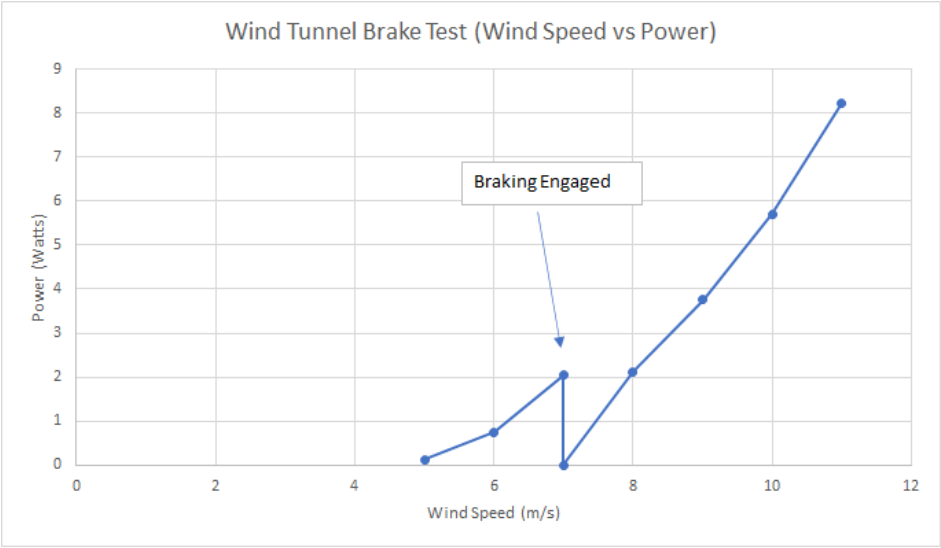

Figure 30. Generative braking wind tunnel test.

Testing of Generator Power Output

The generator was tested throughout the year, first on a dynamometer to test our subsystems and operating plans in the lab, then in the wind tunnel toward the end of the school year to test the combined sub-systems. The wind tunnel allowed for a real-world test of the completed turbine and showcased the mechanical improvements that allowed the axial flux generator to excel. Multiple tests were performed in the wind tunnel where the pitch control, blade design, and braking subsystems were all tested independently and then combined to create the final turbine. Figure 31 shows the power curve in relation to the wind speed tested in the wind tunnel. A smooth progression with a jump to higher voltages can be seen once the wind speed starts to go over 7 m/s. Here we see a relatively low cut in wind speed that our team believes could be improved by further fine tuning of our competition load.

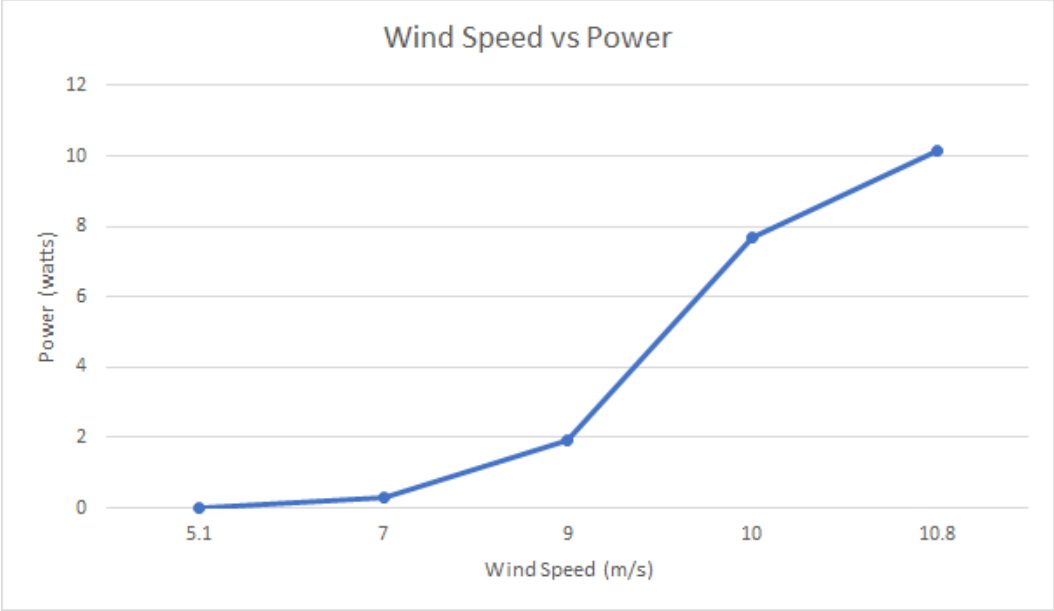

Figure 31. Generator power curve for wind tunnel testing.

Conclusion

This year's competition presented many challenges to our team but with hard work and good communication we were able to have a successful year. Our team learned about the iterative design process with respect to the yaw and pitch control. We learned how to leverage distributed manufacturing to test separate electrical subsystems separately and bring them together in one cohesive unit. We were able to validate these design choices with an iterative testing process which showed that our turbine could produce power meeting the competition requirements. Our successes include designing and implementing an active pitch control system, a voltage regulation system and verifying a generator manufactured by our predecessors. There is still room for improvement with respect to the braking system and yaw control. These systems ran into time or equipment restraints, but we hope our minor success will encourage next year's team. Our last success has been our team's ability to adapt and overcome obstacles as they arrive. This past year has shown the need for flexibility and adaptability, and this competition was no exception.

Appendix A - Pitch Control Script

The pitch control script can be found at the following link:
https://github.com/jcasletonUW/WISCWIND2021/blob/main/Pitch_Control_script.txt

Appendix B - Dynamometer Testing

Preliminary generator testing with different resistive loads was conducted with the team's dynamometer, shown in the graph below.

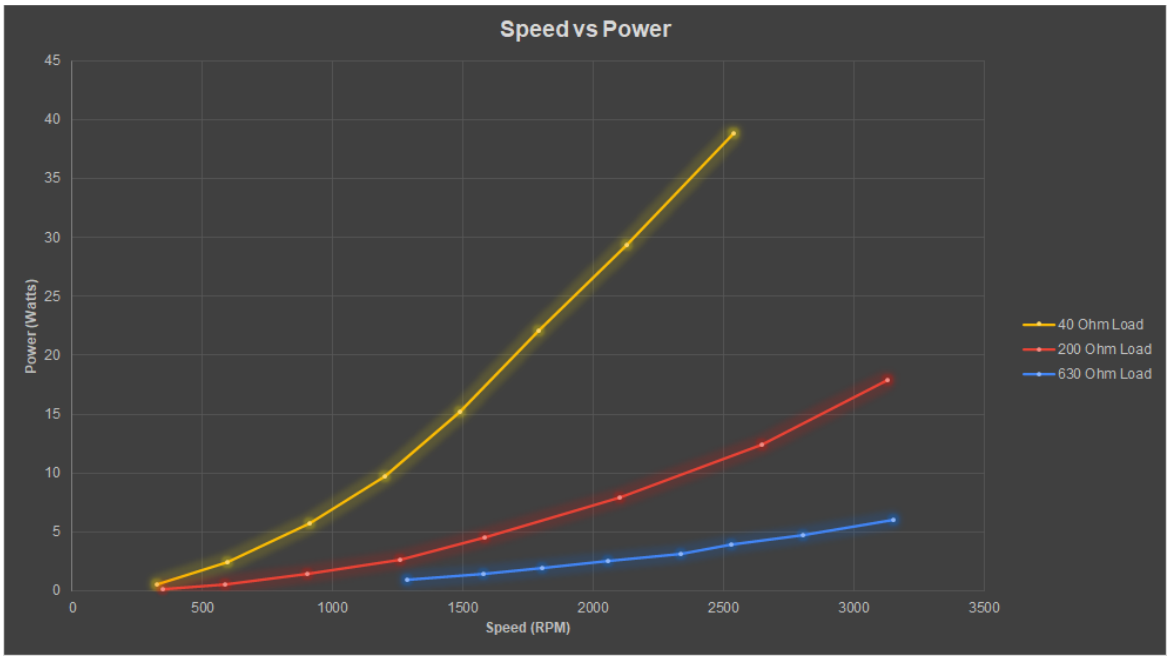

References

[1] Burton T. et al, “Wind Energy Handbook”, *John Wiley & Sons, Ltd*, (2001).

[2] Ellis R. et al, “Design Process for a Scale Horizontal Axis Tidal Turbine Blade,” *Cardiff University*, (Cardiff, United Kingdom, rep., 2018).

[3] Selig, M and McGranahan, B, “Wind Tunnel Aerodynamic Tests of Six Airfoils for Use on Small Wind Turbines” *Department of Aerospace Engineering, University of Illinois at Urbana-Champaign”* November 2004.

[4] Nikhil C. R., Sandip A. K., “Effect of Tail Shapes on Yawing Performance of Micro Wind Turbine,” *International Journal of Energy and Power Engineering, Special Issue: Energy Systems and Developments* (Sept. 2015), Vol. 4, No. 5-1, pp. 38-42. doi: 10.11648/j.ijepe.s.2015040501.16

[5] “Halbach Arrays,” K&J Magnetics. [Online]. Available: https://www.kjmagnetics.com/blog.asp?p=halbach-arrays. [Accessed: 24-Apr-2021].